Dislocation scattering in $Al_xGa_{1-x}N/GaN$ heterostructures

Xiaoqing Xu, Xianglin Liu,[a] Xiuxun Han, Hairong Yuan, Jun Wang, Yan Guo, Huaping Song, Gaolin Zheng, Hongyuan Wei, Shaoyan Yang, Qinsheng Zhu,[b] and Zhanguo Wang

Key Laboratory of Semiconductor Materials Science, Institute of Semiconductors, Chinese Academy of Sciences, P.O. Box 912, Beijing 100083, People's Republic of China

(Received 27 August 2008; accepted 16 October 2008; published online 7 November 2008)

The theoretical electron mobility limited by dislocation scattering of a two-dimensional electron gas confined near the interface of $Al_xGa_{1-x}N/GaN$ heterostructures was calculated. Based on the model of treating dislocation as a charged line, an exponentially varied potential was adopted to calculate the mobility. The estimated mobility suggests that such a choice can simplify the calculation without introducing significant deviation from experimental data, and we obtained a good fitting between the calculated and experimental results. It was found that the measured mobility is dominated by interface roughness and dislocation scattering at low temperatures if dislocation density is relatively high ($>10^9$ cm^{-2}), and accounts for the nearly flattening-out behavior with increasing temperature. © *2008 American Institute of Physics*. [DOI: 10.1063/1.3013836]

Over the past decade or so, the nitride material system has been the focus of intense research.[1–3] $Al_xGa_{1-x}N/GaN$ heterostructures have been an area of active research, owing to the demonstration of high power microwave high electron mobility transistors. Unfortunately, the shortage of lattice-matched substrates leads to high densities (typically 10^8-10^{10} cm^{-2}) of threading dislocations that pass vertically through $Al_xGa_{1-x}N/GaN$ interface.[4] Dislocation scattering has been included in the scattering mechanisms of three-dimensional bulk GaN,[5–8] however, it was not considered in $Al_xGa_{1-x}N/GaN$ two-dimensional electron gas (2DEG)[9,10] until the work of Jena. Jena *et al.* made an initial effort to treat the dislocation scattering in $Al_xGa_{1-x}N/GaN$ 2DEG.[11] Fully considering the screening effect, their model gives a carrier concentration dependence of mobility. A more recent analysis of dislocation scattering in 2DEG was performed by Joshi *et al.*, who used a Monte Carlo method to calculate the deformation potential interaction of electrons from the strain fields surrounding dislocations.[12] The numerical results well describe both the temperature and 2DEG density dependences of electron mobility. However, neither Jena *et al.* nor Joshi *et al.* had adequate experimental data fitted to their work. In this letter, we have grown a series of heterostructure samples, and measured their 2DEG mobilities in the temperature range of 10–300 K. In addition to the experiments, we have also performed a method to calculate the dislocation scattering, and the theoretical results show good agreement with our experimental data.

The samples we consider in this letter were grown on a sapphire substrate using a metal-organic chemical vapor deposition (MOCVD) system. The degreased (0001) sapphire substrate was initially nitrided for about 3 min and subsequently a low-temperature (550 °C) GaN buffer layer with a thickness of 50 nm was grown. Then high-temperature GaN (1000 nm thick), $Al_{0.18}Ga_{0.82}N$ (40 nm thick), and GaN (120 nm thick) were grown sequentially. Two samples (A and B) were selected from several samples grown under similar growth conditions. They were nominally undoped with all the electrons originating from surface states. The 2DEG density in the channel is 6.6×10^{12} cm^{-2}, determined by solving the Poisson and Schrödinger equations self-consistently. Sample parameters were comparable except for the dislocation density and the interface roughness. Hall measurements were performed using the Van der Pauw method in the temperature range of 10–300 K in a closed-loop cryostat. Hot phosphoric and sulfuric acids (3:1 v/v), the so-called orthodox etching method, were used to detect the density of dislocations. Through this processing, etch pits formed on the dislocation sites. Their densities were then determined by atomic force microscopy.

As a dislocation can be considered as a string of charged vacancies in the core,[7] a space charge is formed around it which scatters electrons traveling across it. As the scattering potential of a dislocation is not purely a spatially short range vacancy potential, or a long range Coulomb potential, we proposed an exponentially varied potential $U(r)=-U_0\exp(-r/\beta)$ to replace the exact complicated scattering potential. U_0 is the vacancy potential in the core of the Ga vacancy, which is several tens of eV deep, and here we use 30 eV referring to the calculation result of Baraff and Schlüter.[13] Moreover β, which we call the characterized length, will be determined later. Since the component parallel to the threading dislocations of the scattering potential is considered to be uniform, scattering only happens in the plane perpendicular to the dislocation. The problem should be resolved in a 2D system. The cylindrical coordinates system (z,r,Θ) makes the calculation more convenient, where $r=\sqrt{x^2+y^2}$. Thus, the Hamiltonian matrix element $\langle \boldsymbol{k}'|\boldsymbol{H}|\boldsymbol{k}\rangle$ can be obtained from

$$\langle \boldsymbol{k}'|\boldsymbol{H}|\boldsymbol{k}\rangle = \frac{1}{A}\int U(r)\exp[i(\boldsymbol{k}-\boldsymbol{k}')\boldsymbol{r}]rdrd\Theta, \tag{1}$$

where A is the crystal area perpendicular to the dislocation, $\boldsymbol{k}$ and $\boldsymbol{k}'$ are the initial and final electron wave vectors, respectively, and Θ is the angle between $(\boldsymbol{k}-\boldsymbol{k}')$ and $\boldsymbol{r}$. When taking into account the screening effect, the scattering matrix can be modified by multiply the screening factor, $S(q)$.[14]

[a]Electronic mail: xlliu@red.semi.ac.cn.
[b]Electronic mail: qszhu@semi.ac.cn.

Then, according to Fermi's golden rule, the scattering rate in terms of the transition probability W per unit time is given by

$$W(\mathbf{k}',\mathbf{k}) = \frac{2\pi}{\hbar}|\langle \mathbf{k}'|\mathbf{H}|\mathbf{k}\rangle|^2 S(q)^2 \delta(E_{k'} - E_k)$$
$$= \frac{2\pi}{\hbar}\left|\frac{1}{A}\int_0^\infty U(r)rdr\int_0^{2\pi} \times \exp[i\mathbf{qr}]d\Theta\right|^2 S(q)^2\delta(E_{k'} - E_k), \quad (2)$$

in which

$$S(q) = \frac{q}{q + q_s B(q)}, \quad (3)$$

where $q_s = 2m^*e^2/\varepsilon_s\hbar^2$, with ε_s, m, and e being the dielectric constant, effective electron mass, and electronic charge, respectively. q is the scattering vector, and $q = |\mathbf{k} - \mathbf{k}'| = 2k\sin(\theta/2)$ with θ being the deflection angle of the particles from their original direction of motion, and

$$B(q) = \int_0^\infty dz \int_0^\infty dz' \chi(z)^2\chi(z')^2 \exp(-q|z - z'|), \quad (4)$$

with $\chi(z)$ being the ground-state electron wave function.

Thus, the number of electrons that are scattered with reflecting angles between θ and $\theta + \Delta\theta$ per unit time can be expressed as

$$\Delta n = \left[\frac{A}{(2\pi)^2}\int W(\mathbf{k}',\mathbf{k})k'dk'\right]\Delta\theta. \quad (5)$$

Therefore, the differential cross section $\sigma(\theta)$ can be well defined as

$$\sigma(\theta) = \frac{A\Delta n}{v\Delta\theta} = \frac{A^2}{v(2\pi)^2}\int W(\mathbf{k}',\mathbf{k})k'dk', \quad (6)$$

where v is the electron velocity. Substituting Eqs. (2) and (3) into Eq. (6), and extend the term $\exp[i\mathbf{qr}]$ by the Bessel function, we obtain

$$\sigma(\theta) = \frac{2\pi m^*}{\hbar^3 v}\left|\int_0^\infty U(r)J_0(qr)rdr\right|^2\left[\frac{q}{q + q_s B(q)}\right]^2. \quad (7)$$

In Eq. (7) $J_0(qr)$ is the zero-order Bessel function. Multiplying Eq. (7) by the weighting factor $(1 - \cos\theta)$ and then integrating over all angles, we obtain the total scattering cross section

$$\sigma = \int_0^\pi \sigma(\theta)(1 - \cos\theta)d\theta. \quad (8)$$

For a degenerate electron gas, conduction takes place near the Fermi energy.[15] The wave vector k can be simply set as the Fermi wave vector, $k \approx k_f = \sqrt{2\pi N_s}$,[16] where N_s is the 2DEG concentration. Self-consistent calculation on the Schrödinger and Poisson equations gives the results of about 94% and 6% of electrons populating the ground and the first excited subbands, respectively, at 0 K, and no more than 10% of electrons populate the first excited subband even at 300 K. So we can regard that all electrons populate the ground subband, that is

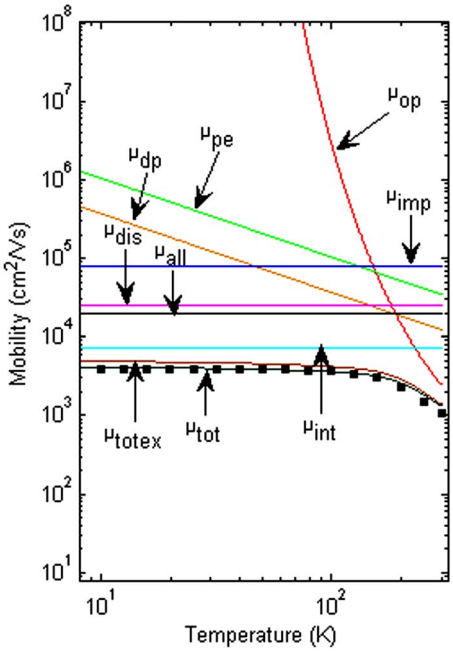

FIG. 1. (Color online) Temperature dependences of theoretical mobilities limited by dislocation scattering together with other standard scattering mechanisms. Experimental data (sample A with a dislocation density of 1.2×10^8 cm^{-2}) are shown by filled squares for a comparison with the calculated total mobility μ_{tot}. The total mobility μ_{totex} clearly deviates from the experimental data.

$$N_s = \frac{m^*k_BT}{\pi\hbar^2}\ln\left[1 + \exp\left(\frac{E_f - E_1}{k_BT}\right)\right], \quad (9)$$

where T, E_f, and E_1 are the temperature, the Fermi energy, and the ground subband energy, respectively.

Finally, the mobility is given by

$$\mu = (e/m^*)[1/N_{dis}v\sigma], \quad (10)$$

where N_{dis} is the density of threading dislocations.

Finally, the characterized length β should be determined, which should be comparable with the GaN lattice constant. By fitting to the experimental data, β is determined to be about 0.3 nm when U_0 is chosen about 30 eV as mentioned before.

Figure 1 shows the calculated temperature-dependent mobilities of different scattering components. In order to fit the experimental data, besides dislocation scattering, six main scattering mechanisms, μ_{op}, μ_{int}, μ_{ii}, μ_{all}, μ_{dp}, μ_{pe}, are introduced, which are the scattering of the optical phonons, interface roughness, ionized impurities, alloy disorder, and acoustic phonons due to both deformation potential and piezoelectric potential, respectively. A total mobility, labeled μ_{tot}, is obtained by using Matthiesen's rule. The experimentally measured mobilities are also depicted in the same figure for a comparison with the calculated results. The dislocation density is 1.2×10^8 cm^{-2}. In order to show how the dislocation scattering reduces the total mobility, we show a calculated total mobility μ_{totex} excluding the mobility component induced by dislocation scattering (μ_{dis}). Obviously, the μ_{totex} deviates from the measured data in the low-temperature region. Thus, we suggest that dislocation scattering should be included during the analysis of the electron mobility in the $Al_xGa_{1-x}N/GaN$ 2DEG.

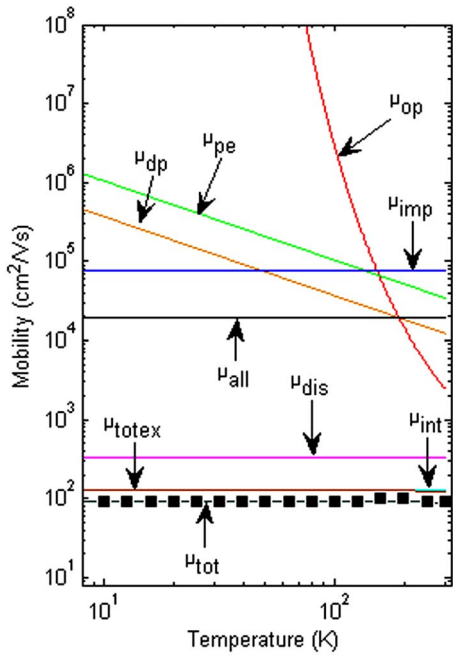

FIG. 2. (Color online) Temperature dependences of theoretical mobilities limited by dislocation scattering together with other standard scattering mechanisms. Experimental data (sample B with a dislocation density of 9.2×10^9 cm^{-2}) are shown by filled squares.

To clarify the dislocation scattering further, we fitted the calculated curves to the experimental data measured on the second sample (sample B) with a dislocation density of 9.2×10^9 cm^{-2} (see Fig. 2). It is found that the measured mobility is dominated by interface roughness and dislocation scattering with a relatively high dislocation density ($>10^9$ cm^{-2}), at low temperatures, and μ_{op} enhances at high temperatures with a trend to dominate the mobility. Our calculation for the interface roughness, ionized impurities, and dislocation scattering rates has been performed in a temperature-independent approximation, and the electron wave vector $\boldsymbol{k}$ is performed at relatively low temperature. However, the approximation does not lose its validity at temperatures below 100 K, for the ground, first excited, and Fermi levels show minor variation. When the temperature exceeds 100 K this approximation will become less valid. However, as is confirmed above, at such temperatures the optical phonon scattering enhances, so our results for total mobilities are still valid.

In conclusion, we have studied the role of the dislocation scattering for a $Al_{0.18}Ga_{0.82}N/GaN$ 2DEG grown by MOCVD technique. Low-temperature (10–100 K) mobility was well fitted with the calculated mobilities induced by interface roughness and dislocation scattering. This mobility was found to be temperature independent, and accounts for the nearly flattening-out behavior at low temperatures. The results explain the phenomenon that low-temperature mobility is enhanced in $Al_xGa_{1-x}N/GaN$ 2DEG upon reduction in dislocation density. The suggested exponentially varied potential seems too rough in describing a real dislocation scattering potential, but is effective in describing the scattering behavior of dislocations in $Al_xGa_{1-x}N/GaN$ heterostructures.

This work was supported by the National Science Foundation of China (Nos. 60506002 and 60776015), the Special Funds for Major State Basic Research Project (973 program) of China (No. 2006CB604907), and the 863 High Technology R&D Program of China (Nos. 2007AA03Z402 and 2007AA03Z451).

[1] R. P. Joshi, Appl. Phys. Lett. **64**, 223 (1994).
[2] S. Nakamura, T. Mukai, and M. Senoh, Appl. Phys. Lett. **64**, 1687 (1994).
[3] R. Gaska, M. S. Shur, A. D. Bykhovski, A. O. Orlov, and G. L. Snider, Appl. Phys. Lett. **74**, 287 (1999).
[4] P. Visconti, K. M. Jones, M. A. Reshchikov, R. Cingolani, H. Morkoc, and R. J. Molnar, Appl. Phys. Lett. **77**, 3532 (2000).
[5] H. M. Ng, D. Doppalapudi, T. D. Moustakas, N. G. Weimann, and L. F. Eastman, Appl. Phys. Lett. **73**, 821 (1998).
[6] N. G. Weimann, L. F. Eastman, D. Doppalapudi, H. M. Ng, and T. D. Moustakas, J. Appl. Phys. **83**, 3656 (1998).
[7] D. C. Look and J. R. Sizelove, Phys. Rev. Lett. **82**, 1237 (1999).
[8] J.-L. Farvacque, Z. Bougrioua, and I. Moerman, Phys. Rev. B **63**, 115202 (2001).
[9] B. K. Ridley, B. E. Foutz, and L. F. Eastman, Phys. Rev. B **61**, 16862 (2000).
[10] M. N. Gurusinghe, S. K. Davidsson, and T. G. Andersson, Phys. Rev. B **72**, 045316 (2005).
[11] D. Jena, A. C. Gossard, and U. K. Mishra, Appl. Phys. Lett. **76**, 1707 (2000).
[12] R. P. Joshi, S. Viswanadha, B. Jogai, P. Shah, and R. D. del Rosario, J. Appl. Phys. **93**, 10046 (2003).
[13] G. A. Baraff and M. Schlüter, Phys. Rev. Lett. **41**, 892 (1978).
[14] L. Hsu and W. Walukiewicz, Phys. Rev. B **56**, 1520 (1997).
[15] J. H. Davies, *The Physics of Low-Dimensional Semiconductors* (Cambridge University Press, Cambridge, 1998).
[16] T. Ando, A. B. Fowler, and F. Stern, Rev. Mod. Phys. **54**, 437 (1982).